ACS Synthetic Biology

pubs.acs.org/synthbio Research Article

A Ribulose-5-phosphate Shunt from the Calvin–Benson Cycle to Methylerythritol Phosphate Pathway for Enhancing Photosynthetic Terpenoid Production

Jie Zhou, Suxian Xu, Hu Li, Huachao Xi, Wenbo Cheng, and Chen Yang*

Cite This: ACS Synth. Biol. 2024, 13, 876–887 Read Online

ACCESS | Metrics & More | Article Recommendations | Supporting Information

ABSTRACT: Cyanobacteria are attractive hosts for photosynthetic terpenoid production, using CO_2 as the sole carbon source. Although the methylerythritol phosphate (MEP) pathway is superior to the mevalonate pathway for cyanobacterial terpenoid synthesis, the first reaction of the MEP pathway, which is catalyzed by 1-deoxy-D-xylulose-5-phosphate (DXP) synthase, involves complex regulation and carbon loss. Here, we constructed a direct route linking ribulose-5-phosphate (Ru5P) in the Calvin–Benson (CB) cycle with DXP in the MEP pathway in a cyanobacterium to increase the terpenoid yield from CO_2 and bypass the DXS-targeted regulations. By employing the adaptive laboratory evolution, we identified new RibB variants including RibB 90–92del with a high activity of synthesizing DXP from Ru5P. These RibB variants were introduced into *Synechococcus elongatus*, resulting in the significantly increased photosynthetic production of isopentenol. The ^{13}C tracer experiments demonstrated a direct carbon flow from Ru5P in the CB cycle to the MEP pathway; thus, this direct route was denoted as the Ru5P shunt. The strain harboring the Ru5P shunt produced 105.2 mg L^{-1} of isopentenol with an average rate of 17.5 mg L^{-1} d^{-1} under continuous light conditions, which is higher than those ever reported for five-carbon alcohol production by photoautotrophic microorganisms. Utilization of the Ru5P shunt in cyanobacterial cells also improved the pinene production, which demonstrates that this shunt can be used to enhance the photosynthetic production of diverse terpenoids.

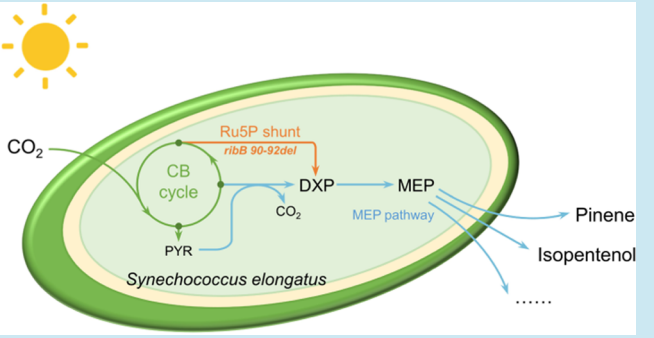

KEYWORDS: *terpenoid, cyanobacteria, CO_2 fixation, metabolic engineering, synthetic biology*

Downloaded via SHANGHAI JIAO TONG UNIV on December 26, 2024 at 05:34:12 (UTC).
See https://pubs.acs.org/sharingguidelines for options on how to legitimately share published articles.

Terpenoids are a large and diverse family of natural compounds found in plants and other free-living organisms.[1,2] They are used as pharmaceuticals, nutraceuticals, fragrances and flavors, agrochemicals, and more recently, potential advanced biofuels.[3,4] For example, isopentenol and pinene, which are hemiterpene alcohol and monoterpene, respectively, are attractive for fuel applications due to their high energy density and low hygroscopicity.[5−7] The universal building blocks of all terpenoids are isopentenyl diphosphate (IPP) and dimethylallyl diphosphate (DMAPP), which can be synthesized via either the mevalonate (MVA) pathway or the methyl-D-erythritol 4-phosphate (MEP) pathway.[8,9] The former pathway is found in archaea, animals, fungi, and plant cytosol, while the latter pathway is present in most bacteria, algae, and plant plastids.

Cyanobacteria are attractive hosts for terpenoid production because they offer the advantage of photosynthetic terpenoid production, using CO_2 as the sole carbon source and sunlight for energy.[10,11] Metabolic engineering has enabled the creation of high-performance cyanobacterial systems that directly convert CO_2 into various terpenoids including hemiterpene isoprene (C5),[12,13] monoterpenes (C10),[14,15] sesquiterpenes (C15),[16,17] and triterpene squalene (C30).[18,19] Our previous study has shown that compared with the MVA pathway, the MEP pathway is superior to the cyanobacterial isoprene synthesis from CO_2 due to a 50% increase in carbon efficiency and relatively large precursor pools.[13] Among the MEP pathway enzymes, 1-deoxy-D-xylulose-5-phosphate (DXP) synthase (DXS) is a key control point in the pathway, which catalyzes the condensation of glyceraldehyde-3-phosphate (GAP) and pyruvate into DXP, with a concomitant loss of CO_2. DXS has been found to be subject to transcriptional and post-translational regulations as well as feedback inhibition by prenyl phosphates.[20] The imbalance in the intracellular supply of GAP and pyruvate may also limit the rate of DXS reaction.[13,21,22] Previous studies have shown that the growth

Received: November 9, 2023
Revised: January 28, 2024
Accepted: February 1, 2024
Published: February 16, 2024

ACS Publications © 2024 American Chemical Society

https://doi.org/10.1021/acssynbio.3c00675
ACS Synth. Biol. 2024, 13, 876–887

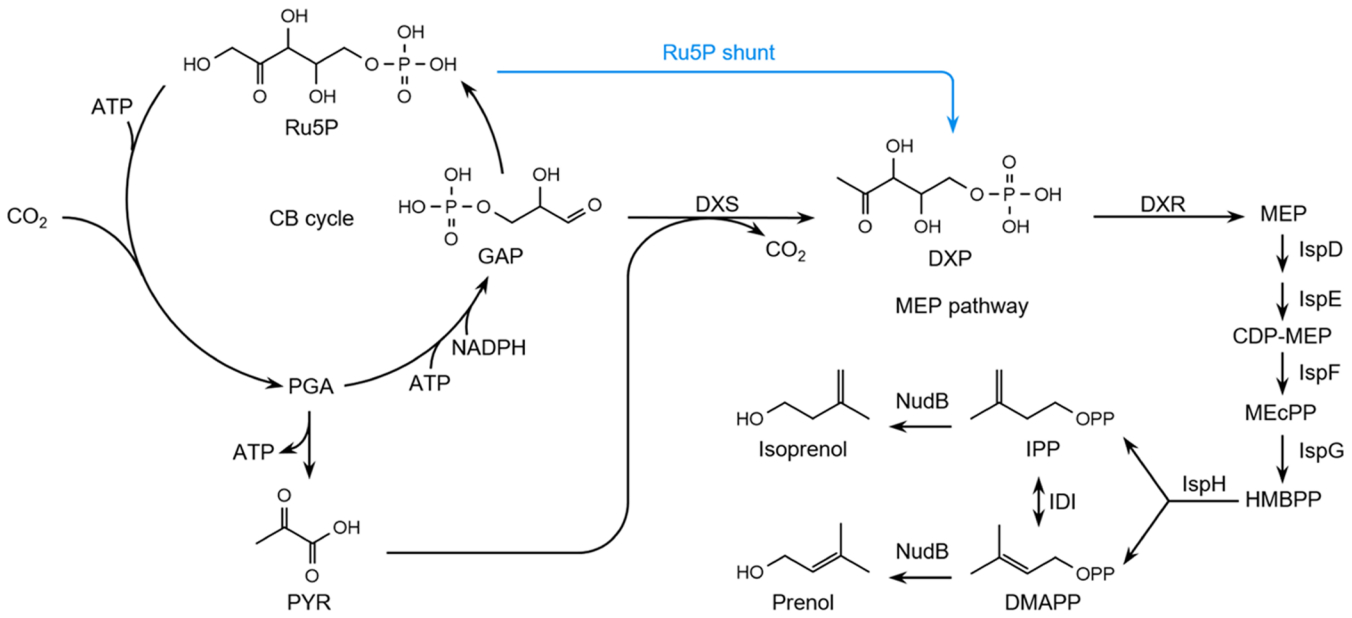

Figure 1. Ru5P shunt for terpenoid synthesis in *S. elongatus*. Pathway intermediates: Ru5P, ribulose-5-phosphate; PGA, 3-phosphoglyceric acid; GAP, glyceraldehyde-3-phosphate; PYR, pyruvate; DXP, deoxyxylulose-5-phosphate; MEP, methylerythritol-4-phosphate; CDP-MEP, diphosphocytidylyl methylerythritol 2-phosphate; MEcPP, methylerythritol 2,4-cyclodiphosphate; HMBPP, 4-hydroxy 3-methylbutenyl diphosphate; IPP, isopentenyl diphosphate; DMAPP, dimethylallyl diphosphate. Enzymes: DXS, DXP synthase; DXR, DXP reductase; IspD, diphosphocytidylyl methylerythritol (CDP-ME) synthase; IspE, CDP-ME kinase; IspF, MEcPP synthase; IspG, HMBPP synthase; IspH, HMBPP reductase; IDI, isopentenyl diphosphate isomerase.

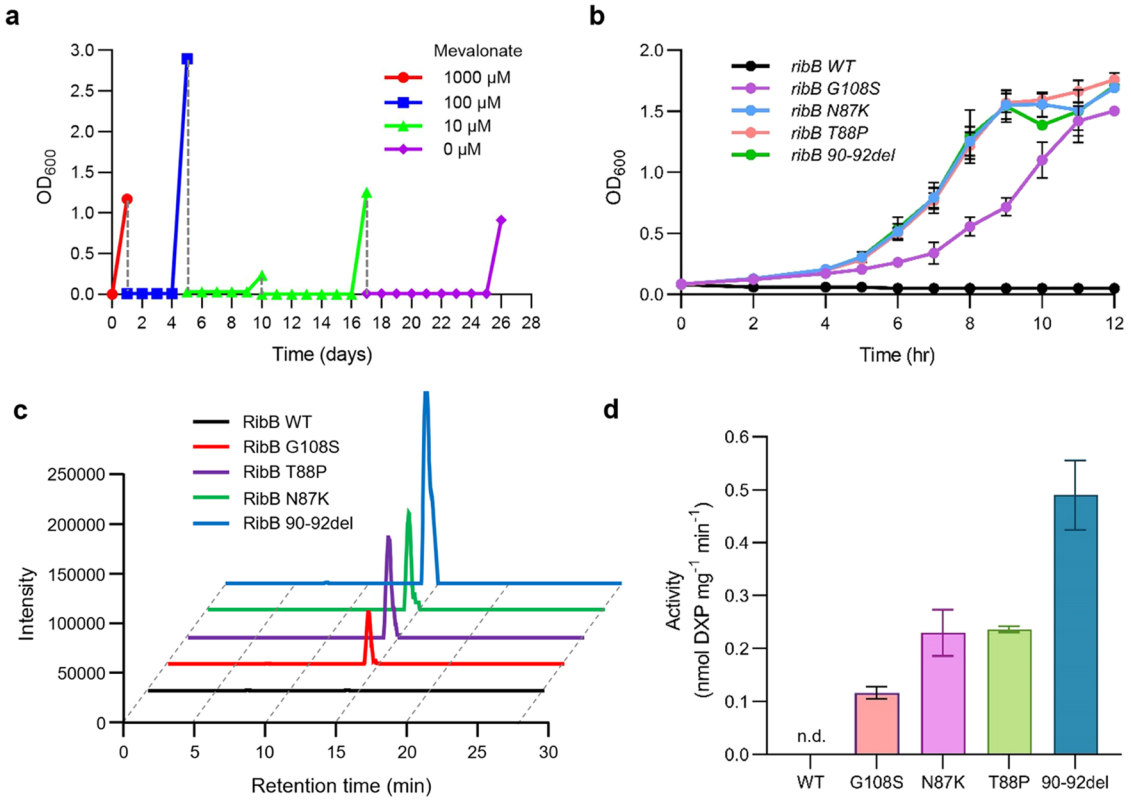

Figure 2. Evolution results and verification of the generated RibB variants. (a) Evolution of the *E. coli* Δ*dxs*Δ*aceE*/pMvaB strain in the medium supplemented with decreasing amounts of mevalonate. The OD_{600} of cultures was monitored. The culture without mevalonate supplementation is indicated by a purple line. (b) Growth curves of *E. coli* Δ*dxs*Δ*aceE*/pMvaB expressing individual *ribB* mutants in the absence of mevalonate. The culture medium contained xylose as a carbon source. The strain overexpressing wild-type *ribB* was used as a control. Data shown are mean ± s.d. (n = 3 independent experiments). (c) LC-MS extracted ion chromatograms (EICs) for DXP (m/z 213.017) produced from the incubation of Ru5P with each of the purified RibB variants. The wild-type RibB was used as a control. (d) DXP-producing activity of the purified RibB variants. Data shown are mean ± s.d. (n = 3 independent experiments). n.d., not detectable.

https://doi.org/10.1021/acssynbio.3c00675
ACS Synth. Biol. 2024, 13, 876−887

Table 1. Mutations in Five Evolved Strains

gene	number of strains	mutation	annotation
clpX	1	G269C	ATP-dependent Clp protease ATP-binding subunit ClpX
fadE	1	A180V	acyl-CoA dehydrogenase
ydaW	1	S158fs[a]	putative uncharacterized protein YdaW
atpD	1	339−349del[b]	ATP synthase F1 complex subunit β
marR	1	L127P	DNA-binding transcriptional repressor MarR
clpP	1	R132H	ATP-dependent Clp protease proteolytic subunit
pcnB	5	R124H	poly(A) polymerase I
malT	5	L822P	DNA-binding transcriptional activator MalT
ribB	5	G108S, T88P, N87K, 90−92del[b]	3,4-dihydroxy-2-butanone-4-phosphate synthase

[a]fs, frameshift. [b]del, in-frame deletion.

of *Escherichia coli* DXS-defective mutants could be rescued by mutations in *aceE* and *ribB* genes, which encode the catalytic E1 subunit of pyruvate dehydrogenase (PDH) complex and the 3,4-dihydroxy-2-butanone 4-phosphate synthase, respectively.[23−25] An RibB mutant, G108S, which was capable of converting ribulose-5-phosphate (Ru5P) to DXP in vitro, has been expressed in *E. coli* and *Pseudomonas putida* for increasing terpene yield from sugars.[25,26]

In this study, we reason that a direct route from a pentose phosphate in the Calvin−Benson (CB) cycle to DXP may increase the terpenoid yield from CO_2 and bypass the DXS-targeted regulations in cyanobacterial cells. By employing adaptive laboratory evolution, we identified new RibB variants with high activities of synthesizing DXP from Ru5P. These RibB variants were expressed in *Synechococcus elongatus* PCC 7942, which resulted in a significant increase in the photosynthetic production of isopentenol. The ^{13}C tracer experiments demonstrated a direct carbon flow from Ru5P in the CB cycle to the MEP pathway. This direct route was denoted as the Ru5P shunt. Utilization of the Ru5P shunt in cyanobacterial cells also improved the photosynthetic production of pinene.

RESULTS

Comparing Ru5P Shunt with Conventional MEP Pathway for Cyanobacterial Terpenoid Synthesis from CO_2. For each DXP synthesized through the conventional MEP pathway, six CO_2 molecules need to be fixed by ribulose 1,5-bisphosphate carboxylase/oxygenase (Rubisco) in the CB cycle, and 11 molecules of NADPH and 16 ATP are required (Figures 1 and S1). By contrast, 5 CO_2 molecules, 10 NADPH, and 15 ATP are required for the synthesis of DXP through the Ru5P shunt. Thus, the Ru5P shunt is more carbon- and energy-efficient than the conventional MEP pathway. Moreover, our previous study showed that the intracellular concentration of GAP was over 30-fold lower than that of pyruvate in *S. elongatus* PCC 7942 growing under light,[13] whereas bacterial DXSs exhibit similar affinities toward both substrates.[27] The availability of GAP may thus limit the terpenoid biosynthetic flux in cyanobacterial cells. On the other hand, the intracellular pentose phosphate pool was relatively abundant (~172.8 μM) in *S. elongatus* PCC 7942 growing in constant light, which was analyzed by liquid chromatography−mass spectrometry (LC−MS). The relatively large pool of pentose phosphates could provide a driving force for terpenoid synthesis through the Ru5P shunt.

Adaptive Evolution in *E. coli* Leads to RibB Mutations. We used the adaptive laboratory evolution approach to isolate genetic mutations for the Ru5P shunt. Previous studies have shown that the mutation in the catalytic E1 subunit of the PDH complex is the most common mechanism to overcome DXS deficiency[23,24] because the mutated PDH could produce 1-deoxy-D-xylulose (DX) from pyruvate and D-glyceraldehyde and DX can then be phosphorylated to DXP by a xylulokinase.[28] Thus, we constructed an *E. coli* Δ*dxs*Δ*aceE* strain harboring the genes for the bottom MVA pathway, which can grow in the presence of exogenously supplied mevalonate and acetate. The strain was cultivated in a medium containing xylose as a carbon source. The amount of supplied mevalonate was sequentially reduced until the cultures could grow in the absence of mevalonate (Figure 2a). From five independent cultures that overcame mevalonate auxotrophy, the clonal strains were isolated and genomically sequenced. All of the strains were found to acquire the mutations in three genes (Table 1). Among these genes, *pcnB* and *malT* encoding poly(A) polymerase I and a transcriptional activator, respectively, have been commonly found to be mutated in previous laboratory evolution experiments,[29,30] and their mutations are not specifically involved in the phenotypic change observed here. Mutations in *ribB* encoding 3,4-dihydroxy-2-butanone 4-phosphate synthase (DHBPS) were identified in all five strains, which included amino acid substitution (G108S, T88P, and N87K) and in-frame deletion (90−92del). Although the G108S mutant of RibB has been characterized previously,[24,25] the latter three mutations in RibB for complementation of DXS deficiency have not been identified before.

We found that the expression of individual *ribB* mutants was sufficient to rescue the growth of *E. coli* Δ*dxs*Δ*aceE* in mevalonate-lacking medium with xylose as a carbon source, whereas the strain overexpressing wild-type *ribB* was unable to grow under the same condition (Figure 2b). Interestingly, the growth rates of the strains expressing *ribB N87K*, *T88P*, and *90−92del* were significantly higher than that of the *rib G108S*-expressing strain. RibB G108S has been shown to convert Ru5P to DXP in vitro.[25] To test whether other RibB variants catalyze the same reaction, we performed biochemical assays using purified recombinant RibB proteins (Figure S2). Incubation of Ru5P with each of the RibB variants N87K, T88P, and 90−92del resulted in the formation of DXP, which was identified by liquid chromatography−mass spectrometry (LC−MS) (Figure 2c). Moreover, the three RibB variants exhibited higher DXP-producing activities than those of RibB G108S (Figure 2d), which is consistent with the observed fast growth of DXS-deficient strains expressing the three variants (Figure 2b). The highest activity of synthesizing DXP from Ru5P was observed for RibB 90−92del (Figure 2d). Similar to RibB G108S,[25] the three RibB variants were incapable of

https://doi.org/10.1021/acssynbio.3c00675
ACS Synth. Biol. 2024, 13, 876−887

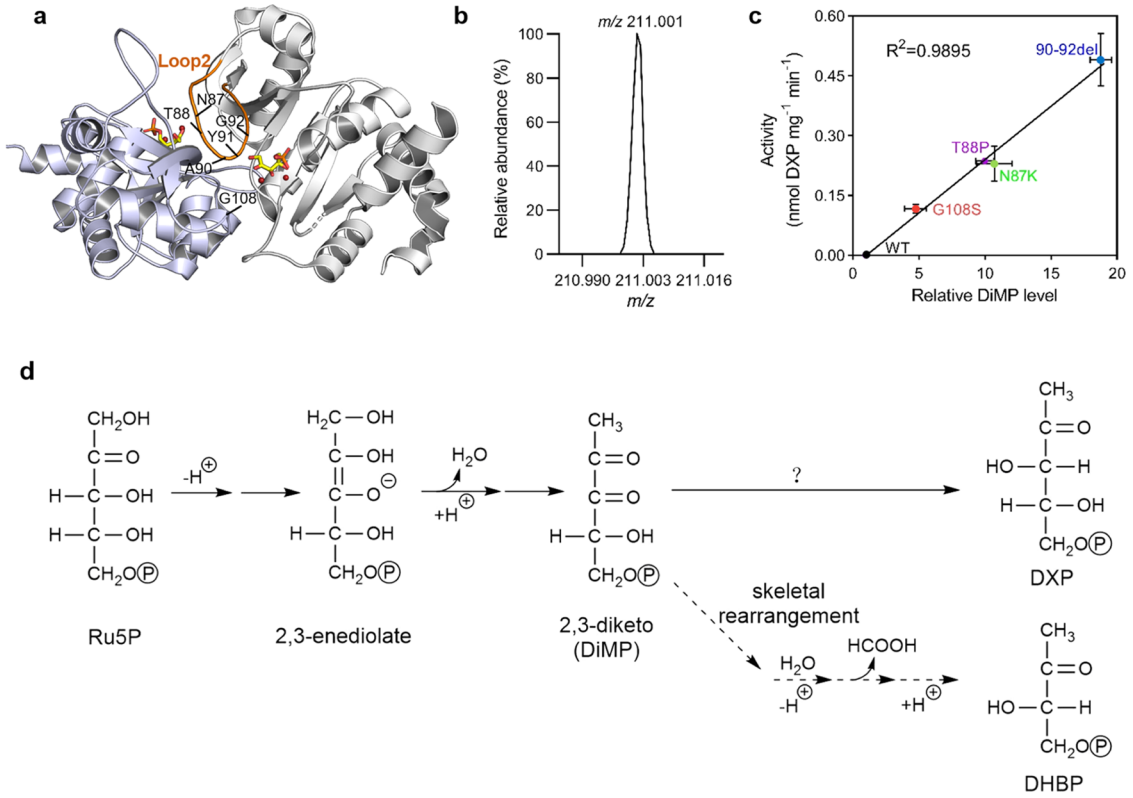

Figure 3. Proposed conversion of Ru5P to DXP by RibB variants. (a) Location of the mutated amino acid residues in the RibB variants. N87, T88, A90, Y91, and G92 are on Loop2 (brown). Homology modeling of *E. coli* RibB was based on the structure of *Vibrio cholerae* RibB in complex with Ru5P and metal ions (Protein Data Bank (PDB), 4P8E). (b) LC-MS analysis of DiMP (m/z 211.001) formed from incubation of Ru5P with RibB variants. (c) Correlation of the DXP-producing activities of individual Ru5P variants and DiMP concentrations in the respective reaction mixtures. (d) Proposed DiMP-involved conversion of Ru5P to DXP. RibB variants could not support the sigmatropic 1,2-skeleton rearrangement of DiMP, resulting in the accumulation of DiMP that is converted to DXP through an unknown mechanism.

converting xylulose-5-phosphate (X5P) or ribose-5-phosphate (R5P) to DXP.

RibB is originally responsible for the conversion of Ru5P to formate and 3,4-dihydroxy-2-butanone 4-phosphate (DHBP), the latter of which is a biosynthetic precursor of riboflavin.[31] Among RibB proteins from diverse sources, amino acid residues N87, T88, A90, Y91, and G92 are highly conserved. These residues are located on Loop2 of DHBPS (Figure 3a). Previous studies have shown that the closing of Loop2 with an ordered conformation, which was observed in the presence of Ru5P and metal ions, is essential for the catalytic activity of DHBPS.[32] The G108 residue has also been found to be critical for the closed conformation of Loop2.[33] Thus, we speculate that mutations of N87, T88, A90, Y91, G92, and G108 may change the complex of DHBPS with Ru5P and metal ions, leading to diminished formation of DHBP and the release of the reaction intermediates. Indeed, we observed the accumulation of a compound with a mass-to-charge ratio (m/z) of 211.001 in the reaction mixture containing the RibB variants and Ru5P (Figure 3b). Moreover, the DXP-producing activities of individual RibB variants and the concentrations of the m/z = 211.001 compound in the respective reaction mixtures were strongly and positively correlated (Figure 3c). This compound is probably the 2,3-diketo intermediate of the DHBPS reaction, 1-deoxy-D-glycero-2,3-pentodiulose 5-phosphate (DiMP), which is generated from Ru5P through enolization, protonation, and dehydration (Figure 3d).[34] Therefore, the mutations in RibB might result in the binding of Ru5P to metal ions in incompact conformation, which could not support the sigmatropic skeletal rearrangement of DiMP for generation of the final products, formate and DHBP.[34] DiMP is thus accumulated and reduced to form DXP (Figure 3d).

Introduction of RibB Variants into *S. elongatus* for Improving Isopentenol Production. To construct the Ru5P shunt for cyanobacterial isopentenol production, the gene encoding *E. coli* NudB along with each *ribB* mutant was expressed under the control of P_{trc} promoter and integrated into the genome of *S. elongatus* PCC 7942 (Figure S3). The isopentenol, including isoprenol and prenol, can be formed from dephosphorylation of IPP and DMAPP by the Nudix hydrolase NudB (Figure 1).[5] We cultivated the recombinant *S. elongatus* strains in BG-11 medium containing $NaHCO_3$ under continuous light and measured isopentenol production and cell growth. Among these strains, the best producer was strain SI02 expressing *nudB* and *ribB 90−92del*, which showed a 1.9-fold higher rate of isopentenol production than strain SI01 expressing *nudB* only (Figure 4a). Expression of other *ribB* mutants (*G108S*, *T88P*, and *N87K*) also significantly increased the isopentenol production. A slight reduction of cell growth rate was observed for the strains expressing *nudB* and *ribB* mutants compared to strain SI01 (Figure 4b). In contrast, the strain overexpressing *dxs* showed severely impaired cell growth, although the cellular isopentenol productivity of this strain was comparable to that of strain SI02. The growth impairment of the *dxs*-overexpressing strain could be due to the accumulation of MEP pathway intermediates and the depletion of GAP and other central carbon metabolites (Figure S4).

https://doi.org/10.1021/acssynbio.3c00675
ACS Synth. Biol. 2024, 13, 876−887

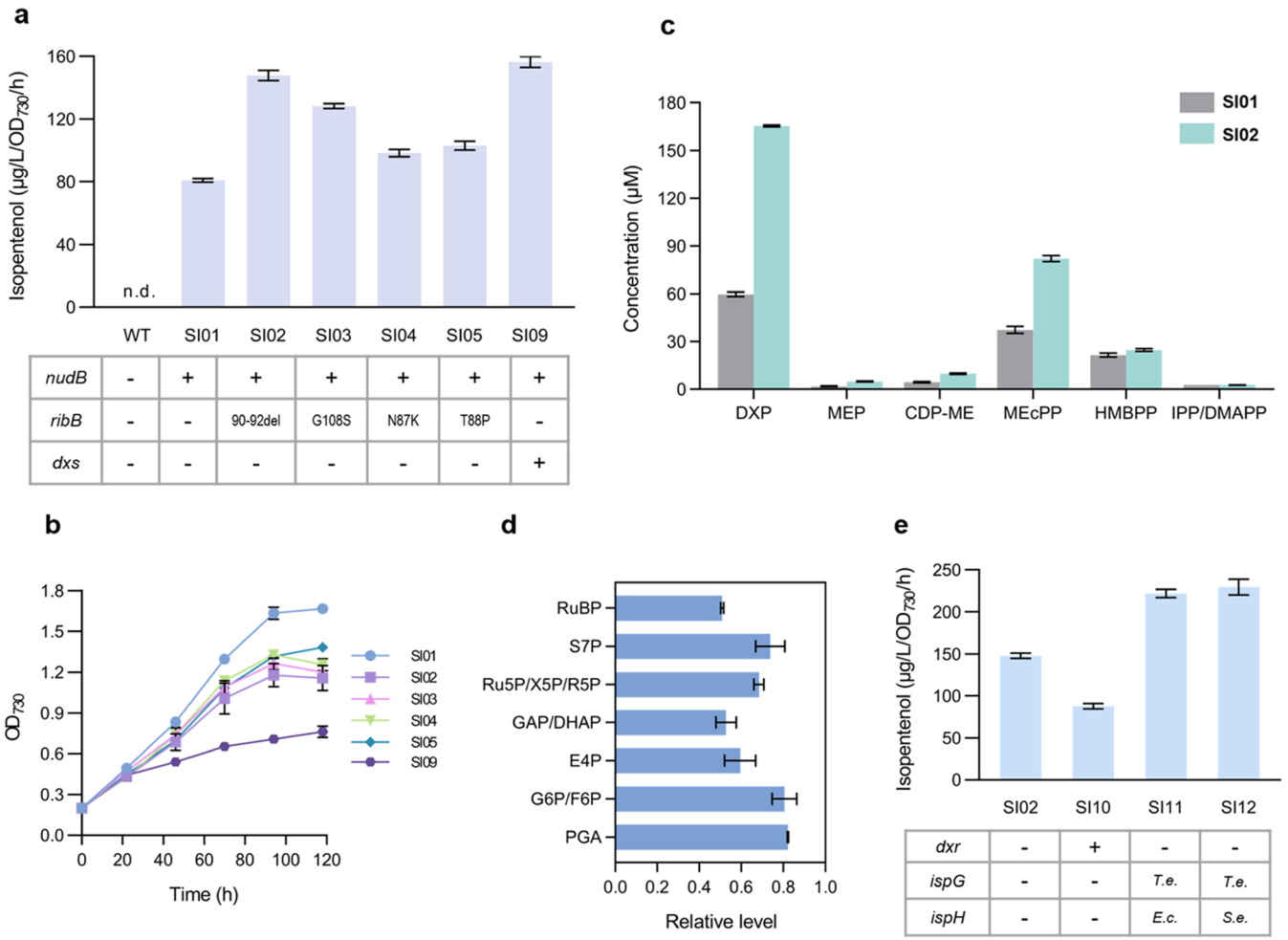

Figure 4. Construction of the Ru5P shunt for improving isopentenol production in *S. elongatus*. (a) Isopentenol production by *S. elongatus* strains expressing *nudB* with individual *ribB* mutants. The *nudB* row indicates the inclusion (+) of *E. coli nudB* or absence (−) of the gene. The *ribB* row indicates the expressed *ribB* mutant or the absence (−) of the mutated *ribB*. The *dxs* row indicates the overexpression of endogenous *dxs* (+) or not (−). The wild-type *S. elongatus* did not produce a measurable amount of isopentenol. (b) Growth curves of *S. elongatus* strains. (c) Intracellular concentrations of MEP pathway intermediates in strain SI01 expressing *nudB* only and strain SI02 expressing *nudB* with *ribB 90−92del*. IPP and DMAPP were not differentiated by the LC-MS method used. (d) Relative concentrations of CB cycle intermediates in the strain SI02 compared to those in the strain SI01. G6P and F6P, GAP and dihydroxyacetone phosphate (DHAP), as well as Ru5P, X5P, and R5P were not differentiated by the LC-MS method used. S7P, sedoheptulose-7-phosphate; E4P, erythrose-4-phosphate. (e) Effect of overexpression of *dxr*, *ispG*, and *ispH* on isopentenol production by the strains expressing *nudB* with *ribB 90−92del*. The *dxr* row indicates the overexpression of endogenous *dxr* (+) or not (−). The *ispG* and *ispH* rows indicate the source organism for the gene or the absence of the exogenous gene (−). *T.e.*, *Thermosynechococcus elongatus*; *E.c.*, *E. coli*; and *S.e.*, *S. elongatus*. Data shown in panels a−e are mean ± s.d. (n = 3 independent experiments).

To obtain a comprehensive view of the metabolic consequence of the introduction of RibB variants, we compared intracellular metabolomes between the strains SI02 and SI01. The intracellular concentrations of the MEP pathway intermediates including DXP, MEP, 4-diphosphocytidyl methyl-D-erythritol (CDP-ME), and methylerythritol 2,4-cyclodiphosphate (MEcPP) were increased 2.2−2.8 fold by expression of the *ribB* mutant (Figure 4c). Thus, the introduction of the RibB variant probably increased the carbon flux through the MEP pathway, leading to enhanced isopentenol production in *S. elongatus*. On the other hand, the expression of *ribB* mutant had only a modest effect on the pools of the CB cycle intermediates (Figure 4d). Particularly, the intracellular concentrations of Ru5P, R5P, and X5P were not changed significantly in strain SI02 compared to those in strain SI01.

To further increase the MEP pathway flux toward isopentenol synthesis, we overexpressed the *dxr*, *ispG*, and *ispH* genes, which encode DXP reductase, 4-hydroxy-3-methylbut-2-enyl-diphosphate synthase, and 4-hydroxy-3-methylbut-2-enyl-diphosphate reductase, respectively, due to the substantial accumulation of DXP and MEcPP in strain SI02. The strain overexpressing *dxr* did not show an increase in isopentenol production compared to strain SI02. However, the overexpression of both *ispG* and *ispH* significantly enhanced isopentenol production (Figure 4e). A 1.6-fold increase in the isopentenol production rate was observed for strain SI12 overexpressing *ispG* from *T. elongatus* BP-1 and endogenous *ispH* compared to strain SI02.

^{13}C-Labeling Experiments Confirm the Operation of the Ru5P Shunt. To confirm the activity of the Ru5P shunt in vivo, we conducted ^{13}C-labeling experiments using [^{13}C]-bicarbonate or uniformly labeled (*U*) [*U*-^{13}C]glucose as tracers. The cultures of *S. elongatus* strain SI01 expressing *nudB* only and strain SI02 expressing *nudB* with *ribB 90−92del* were supplemented with [^{13}C]bicarbonate under continuous

https://doi.org/10.1021/acssynbio.3c00675
ACS Synth. Biol. 2024, 13, 876−887

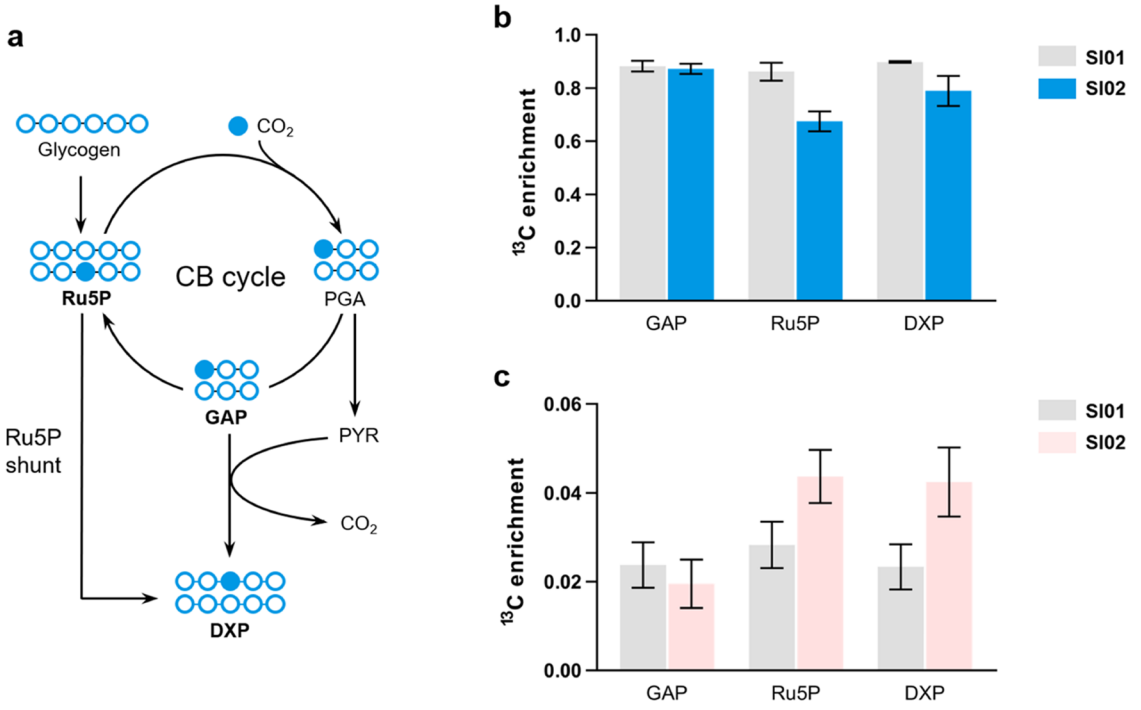

Figure 5. ^{13}C-labeling experiments show the carbon flow through the Ru5P shunt. (a) Schematic of [^{13}C]bicarbonate-derived labeling through the CB cycle. Labeled carbon atoms are marked by a solid circle. (b) Steady-state ^{13}C enrichment of GAP, Ru5P, and DXP in *S. elongatus* strain SI01 expressing *nudB* only and strain SI02 expressing *nudB* with *ribB 90−92del*. The strains were grown in [^{13}C]bicarbonate medium under continuous light. (c) Steady-state ^{13}C enrichment of GAP, Ru5P, and DXP derived from [*U*-^{13}C]glucose in strains SI01 and SI02. The strains were growing in BG-11 medium under light conditions and then switched to [*U*-^{13}C]glucose medium under the dark condition. Data shown in panels b and c are mean ± standard deviation (n = 3 independent experiments).

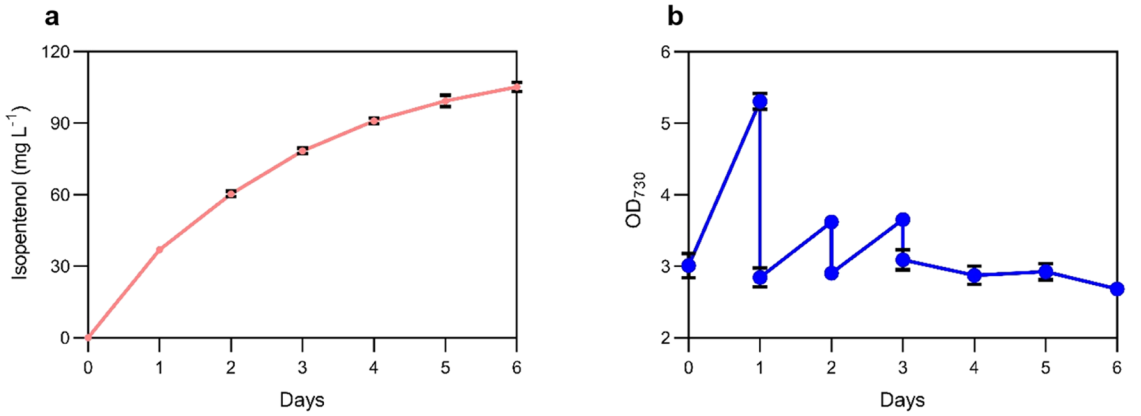

Figure 6. Long-term photosynthetic isopentenol production. The strain SI12 was cultured in a modified BG-11 medium containing 100 mM of $NaHCO_3$ under continuous light. Cells were induced with 1 mM of IPTG on day 0. On days 1, 2, and 3, cells were collected and resuspended in fresh medium to an OD_{730} of 3.0. Cumulative isopentenol production (a) and cell growth (b) were determined. Data shown are mean ± s.d. (n = 3 independent experiments).

light. At various time points after tracer administration, intracellular metabolites were rapidly extracted and then analyzed by LC-MS. Through the reaction catalyzed by carbonic anhydrase, [^{13}C]bicarbonate was converted to $^{13}CO_2$, which was subsequently assimilated through the CB cycle (Figure 5a). We observed that the ^{13}C label was incorporated into the CB cycle intermediates, reaching the isotopic steady state within 4 min. The extent of Ru5P labeling was lower in strain SI02 than that in strain SI01 (Figure 5), which is probably due to the metabolic flux of glycogen into Ru5P through the glycogen catabolic pathway and the oxidative pentose phosphate pathway.[35,36] Consistently, the intermediates of both pathways, including glucose-6-phosphate (G6P), fructose-6-phosphate (F6P), and 6-phosphogluconate, were also less labeled in strain SI02 than in strain SI01. We found that the ^{13}C enrichments of GAP and DXP were similar in strain SI01 (Figure 5b), which is consistent with DXP synthesis from GAP and pyruvate. By contrast, the extent of DXP labeling was significantly lower than that of GAP in strain SI02, indicating that the carbon flow through the Ru5P shunt resulted in a decrease in the labeled fraction of DXP.

Although *S. elongatus* is an obligate photoautotroph, it can take up exogenous glucose with a low rate.[37] We switched photosynthetic cyanobacterial cells to medium containing

https://doi.org/10.1021/acssynbio.3c00675
ACS Synth. Biol. 2024, 13, 876−887

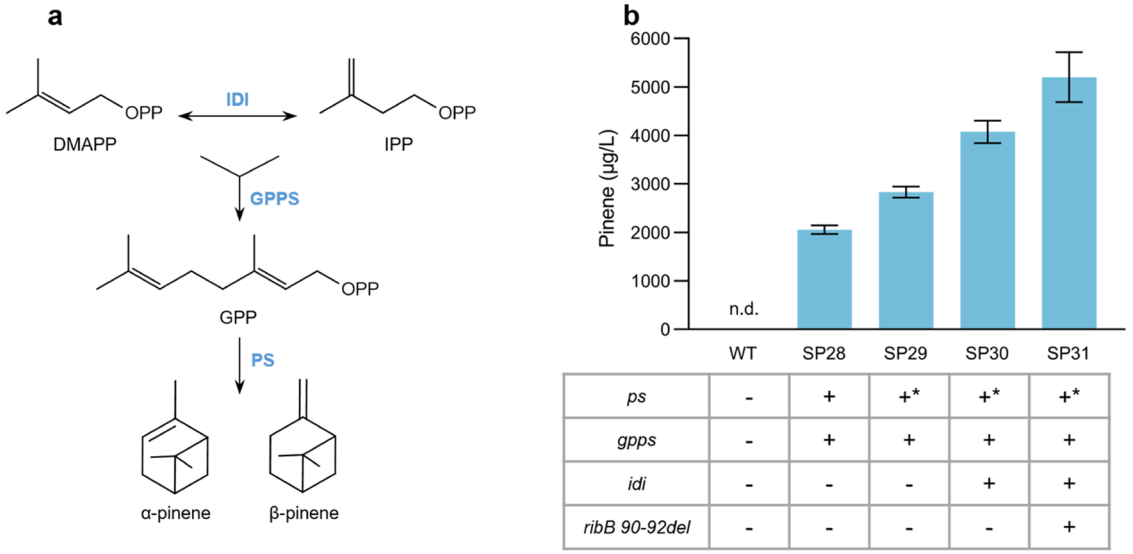

Figure 7. Utilization of the Ru5P shunt for enhancing pinene production in *S. elongatus*. (a) The biosynthetic pathway of pinene. (b) Pinene production by *S. elongatus* strains. The *ps* row indicates the expression of codon-optimized *A. grandis ps* (+), the *ps Q456L* mutant (+*), or the absence (−) of the gene. The *gpps* row indicates inclusion (+) of codon-optimized *A. grandis gpps* or absence (−) of the gene. The *idi* row indicates the expression of *S. cerevisiae idi* (+) or not (−). The *ribB 90−92del* row indicates the expression of the *ribB* mutant (+) or not (−). Data shown are mean ± s.d. (n = 3 independent experiments).

[*U*-^{13}C]glucose in the dark. The dark condition was used to reduce the dilution of ^{13}C label in central metabolites from CO_2. The central metabolites reached the isotopic steady state within 4 h under this condition. [*U*-^{13}C]glucose was routed through the oxidative pentose phosphate pathway, resulting in the formation of labeled Ru5P.[38,39] We observed that the extent of Ru5P labeling was higher in strain SI02 than that in strain SI01, whereas the ^{13}C enrichment of GAP was similar in both strains (Figure 5c). Interestingly, DXP was significantly more labeled than GAP and the ^{13}C-labeled fractions of DXP and Ru5P were similar in strain SI02. Together, the results of the ^{13}C-labeling experiments demonstrate carbon flow through the Ru5P shunt in the *S. elongatus* strain expressing RibB 90−92del.

Long-Term Photosynthetic Isopentenol Production through the Ru5P Shunt and MEP Pathway. We cultivated the leading strain SI12 expressing *nudB*, *ribB 90−92del*, *ispG*, and endogenous *ispH* from the P_{trc} promoter in the BG-11 medium containing 100 mM $NaHCO_3$ for 6 days under continuous illumination (Figure 6). The concentrations of A5 trace metals (Mn^{2+}, Zn^{2+}. Co^{2+}, Cu^{2+}, BO_3^{3-}, MoO_4^{2-}) in medium were increased to improve cofactor availability.[40] Cumulative isopentenol production of strain SI12 reached 105.2 mg L^{-1} on day 6 (Figure 6), which is higher than those ever reported for five-carbon alcohol production by photoautotrophic microorganisms.[41] The average rate of the photosynthetic isopentenol production throughout cultivation was 17.5 mg L^{-1} d^{-1}.

Utilization of the Ru5P Shunt for Photosynthetic Pinene Production. To test whether the utilization of the Ru5P shunt could improve the production of other terpenoids, we constructed pinene-producing *S. elongatus* strains expressing RibB 90−92del (Figure 7). The pinene synthase (PS) and geranyl diphosphate synthase (GPPS) from *Abies grandis* were introduced into *S. elongatus*, both of which were codon-optimized and fused with a short ubiquitin-like modifier (SUMO) tag to enhance their expression in cyanobacterial cells.[42] Consistent with a previous report,[43] pinene production was improved by the expression of the PS Q456L variant with distinct metal dependency. A further increase in pinene production was observed for strain SP30 expressing IPP isomerase from *Saccharomyces cerevisiae*. We introduced RibB 90−92del into strain SP30, generating strain SP31 (Figure 7). The strain SP31 produced 5.2 mg L^{-1} of pinene, which is 28% higher than that of SP30 (4.1 mg L^{-1}). Therefore, utilization of the Ru5P shunt enhanced the photosynthetic production of pinene in *S. elongatus*.

DISCUSSION

In this study, we constructed the Ru5P shunt linking the CB cycle with the MEP pathway directly in cyanobacterium *S. elongatus* for the photosynthetic production of terpenoids from CO_2. The carbon flow through the constructed Ru5P shunt in cyanobacterial cells was revealed by [^{13}C]bicarbonate and [*U*-^{13}C]glucose labeling experiments. The strain harboring the Ru5P shunt produced 105.2 mg L^{-1} of isopentenol under continuous light conditions, which is higher than those ever reported for five-carbon alcohol production by photoautotrophic microorganisms. We demonstrated that the utilization of the Ru5P shunt also enhanced the photosynthetic production of pinene in *S. elongatus*. Compared with the introduction of the Ru5P shunt, the overexpression of DXS in *S. elongatus* resulted in a severe impairment in cell growth, which could be partly due to the depletion of GAP and other central carbon metabolites. The limited availability of GAP for terpenoid biosynthesis has also been reported for *E. coli* and other bacteria.[13,21,22] Moreover, the Ru5P shunt is more carbon- and energy-efficient than the conventional MEP pathway; thus, the utilization of the Ru5P shunt allows a higher maximum photosynthetic productivity of terpenoids.

Here, we report the laboratory evolution of previously unidentified RibB variants for the Ru5P shunt. These RibB variants, especially 90−22del, showed high activities of synthesizing DXP from Ru5P. However, the RibB variants are still capable of converting Ru5P to formate and DHBP, though the activities are much lower than that of the wild-type

https://doi.org/10.1021/acssynbio.3c00675
ACS Synth. Biol. 2024, 13, 876−887

enzyme. We attempted to merge the mutations in RibB, but the resulting mutants did not show higher DXP-synthesizing activities in comparison to RibB 90−22del. Extensive protein engineering of RibB is required to completely terminate the original reaction and increase the DXP-synthesizing activity. Based on the strong positive correlation between the DXP-producing activities of Ru5P variants and DiMP concentrations in vitro, we propose that the RibB variants could not support the sigmatropic skeleton rearrangement of DiMP, resulting in the accumulation of DiMP. However, how DiMP is reduced to form DXP remains unknown and requires further investigation. According to previous studies, DiMP is a Rubisco mutant-catalyzed reaction product that is formed from the elimination of phosphate from the enediol of ribulose 1,5-bisphosphate (RuBP).[44] Whether the conversion of RuBP to DXP might be achieved from the engineering of Rubisco enzymes is an intriguing question and worth further studies.

The MEP pathway enzymes IspG and IspH were identified as bottlenecks for further improving isopentenol production in *S. elongatus* harboring the Ru5P shunt. Overexpression of both IspG and IspH significantly increased the isopentenol biosynthetic flux. In contrast, the overexpression of IspG only resulted in the accumulation of the intermediate 4-hydroxy-3-methylbut-2-enyldiphosphate (HMBPP) and did not enhance the isopentenol production. Similar results have been reported for β-carotene-producing *E. coli*.[45] Previous studies have shown that the overexpression of the RibB G108S and DXP reductase (DXR) enzyme fusion improved the bisabolene production in *E. coli* and the α-humulene production in *Methylotuvimicrobium alcaliphilum*.[25,46] However, we did not observe an increase in isopentenol production in *S. elongatus* strains overexpressing RibB variant and DXR separately or their fusion when compared to the strain overexpressing the RibB variant. In fact, the overexpression of DXR in *S. elongatus* resulted in the accumulation of MEP pathway intermediates including MEP and HMBPP as well as severely impaired cell growth. Unraveling the regulatory mechanisms that control terpenoid biosynthesis via the Ru5P shunt and MEP pathway in cyanobacterial cells could allow us to further improve the photosynthetic terpenoid production.

The Ru5P shunt provides an example of a direct link between carbon fixation and the biosynthetic pathway of target compounds in photoautotrophic organisms. Ru5P is interconverted to R5P by R5P isomerase, and R5P is a precursor for the synthesis of histidine and nucleotides. To avoid the competition for the central carbon metabolites, cell density-dependent dynamic regulatory systems could be developed to decouple cell growth with target compound production.[47] We observed that the high-cell-density culture of recombinant *S. elongatus* produced isopentenol at a high rate during long-term cultivation. Further enhancement in photosynthetic isopentenol production might be achieved by autonomous down-regulation of histidine, nucleotide, and riboflavin biosynthesis when the cyanobacterial cultures reach a high density.

MATERIALS AND METHODS

Strains and Plasmids. *S. elongatus* PCC 7942 strains used in this study are shown in Table 2. The plasmids used in this study are listed in Table S1.[13,48] Transformation of *S. elongatus* PCC 7942 was performed as described previously.[49] Integration of the target genes in the neutral site II (NSII)[50] or NSIII[51] in the genome was verified by PCR analysis and DNA sequencing. Complete chromosomal segregation for the introduced DNA fragments was confirmed by PCR (Figure S3).

Table 2. *S. elongatus* PCC 7942 Strains Were Used in This Study

strain	description	reference
WT	Wild-type *S. elongatus* PCC 7942	ATCC
SI01	WT NSII::P_{trc} $nudB_{E.c.}$	this study
SI02	WT NSII::P_{trc} $nudB_{E.c.}$ $ribB_{E.c.}$90−92*del*	this study
SI03	WT NSII::P_{trc} $nudB_{E.c.}$ $ribB_{E.c.}$*G108S*	this study
SI04	WT NSII::P_{trc} $nudB_{E.c.}$ $ribB_{E.c.}$*N87K*	this study
SI05	WT NSII::P_{trc} $nudB_{E.c.}$ $ribB_{E.c.}$*T88P*	this study
SI09	WT NSII::P_{trc} $nudB_{E.c.}$ $dxs_{S.e.}$	this study
SI10	WT NSII::P_{trc} $nudB_{E.c.}$ $ribB_{E.c.}$90−92*del* $dxr_{S.e.}$	this study
SI11	WT NSII::P_{trc} $nudB_{E.c.}$ $ribB_{E.c.}$90−92*del* $ispG_{T.e.}$ $ispH_{E.c.}$	this study
SI12	WT NSII::P_{trc} $nudB_{E.c.}$ $ribB_{E.c.}$90−92*del* $ispG_{T.e.}$ $ispH_{S.e.}$	this study
SP28	WT NSII::P_{trc} $ps_{A.g.}$ $gpps_{A.g.}$	this study
SP29	WT NSII::P_{trc} $ps_{A.g.}$*Q456L* $gpps_{A.g.}$	this study
SP30	SP29 NSIII::P_{trc} $idi_{S.c.}$	this study
SP31	SP29 NSIII::P_{trc} $idi_{S.c.}$ $ribB_{E.c.}$90−92*del*	this study

Growth Conditions. *S. elongatus* strains were routinely grown at 30 °C in BG-11 medium[52] with rotary shaking (180 rpm) and continuous light (55 μmol of photons m^{-2} s^{-1}). Cells were precultured to an optical density at 730 nm (OD_{730}) of ∼1.0 and resuspended in 50 mL of fresh BG-11 medium containing 100 mM $NaHCO_3$ in 250 mL shake flasks to an OD_{730} of ∼0.2. When the cultures were grown to an OD_{730} of ∼0.5, isopropyl-β-D-thiogalactopyranoside (IPTG; 1 mM) was added. Cell growth was monitored by measuring OD_{730}. *E. coli* MG1655 *dxs*- and *aceE*-deleted strains expressing individual variants of RibB were grown in EZ-rich medium (Teknova) containing 1% D-xylose as a carbon source (EZ-X), and OD_{600} was measured throughout the cultivation.

Laboratory Evolution Experiment. *E. coli* MG1655 *dxs*- and *aceE*-knockout strain harboring the pMvaB plasmid encoding mevalonate kinase from *Methanosarcina mazei*, phosphomevalonate kinase, mevalonate pyrophosphate decarboxylase, and isopentenyl pyrophosphate isomerase from *S. cerevisiae*[53] were used for evolution experiments. The strain was grown overnight in the LB medium containing 25 μg mL^{-1} of chloramphenicol. The overnight culture was used to inoculate 1:100 into 2 mL of EZ-X medium containing mevalonate (1 mM), potassium acetate (2 mM), and chloramphenicol (25 μg mL^{-1}). If growth exceeded OD_{600} of 1.0, the strain was passed into the fresh medium at a 1:100 dilution. The concentration of mevalonate in the medium was reduced to 10-fold. When mevalonate was reduced to 10 μM, cells were passed into the medium without mevalonate supplementation if the OD_{600} exceeded 1.0. If the culture grew, aliquots were streaked onto EZ-X agar lacking mevalonate. The phenotype of growing colonies was reconfirmed by growth in a liquid medium without mevalonate supplementation. The isolated strains were submitted to GENEWIZ Inc. for genome sequencing using parent strain Δ*dxs*Δ*aceE*/pMvaB as a reference.

Protein Expression and Purification. Coding sequences for RibB and its variants, G108S, 90−92del, N87K, and T88P, were cloned into pET28a. The resulting plasmids were used to produce the respective proteins with an N-terminal hexahistidine tag. *E. coli* BL21Rosetta(DE3) (Novagen) was transformed with individual expression plasmids and grown at 37 °C in the LB medium. IPTG (0.5 mM) was added to cultures at an OD_{600} of ∼0.8, and then cells were cultivated at 16 °C for

https://doi.org/10.1021/acssynbio.3c00675
ACS Synth. Biol. 2024, 13, 876−887

18 h. After the cells were harvested, protein purification by nickel-nitrilotriacetic acid affinity chromatography was performed as described previously.[54] The purities of proteins were checked by SDS-PAGE (Figure S2).

Enzyme Assay. To test the DXP-producing activity of the RibB variants, the purified enzyme (20 μg) and Ru5P (5 mM) were added to 200 μL of 50 mM tris−HCl buffer, pH 7.5, containing 150 mM NaCl, 10 mM $MgCl_2$, and 5 mM dithiothreitol. After the mixture was incubated at 37 °C for 30 min, 200 μL of methanol was added to stop the reaction. DXP and 1-deoxy-D-glycero-2,3-pentodiulose 5-phosphate (DiMP) produced by the enzymatic reaction were analyzed by LC-MS.

Terpene Production in *S. elongatus*. *S. elongatus* strains were grown at 30 °C in 100 mL shake flasks with 30 mL of BG-11 medium containing 100 mM $NaHCO_3$ under continuous light (55 μmol of photons m^{-2} s^{-1}). After the addition of 1 mM IPTG at an OD_{730} of ∼0.5, the cultures were grown for 24 h. Subsequently, the cells were washed and resuspended in 5 mL of fresh medium to an OD_{730} of 3.0 in 15 mL sealed tubes. After 6 h of cultivation with constant illumination, the cultures were sampled for isopentenol measurements. Addition of an overlay of oleyl alcohol (1 mL) to cultures did not increase the detected isopentenol content, which indicates that isopentenol evaporation could be negligible in our production assays.[55] For the production of pinene, the cultures were performed in the same way as those for isopentenol production except the addition of an overlay of tetradecane (1 mL) to 5 mL of medium in sealed tubes. After 10 h of cultivation with continuous light, samples were collected in the tetradecane overlay for pinene measurements.

For long-term production of isopentenol, the cultures were grown with an initial OD_{730} of 3.0 in 25 mL of BG-11 medium in plug-sealed tissue culture flasks (75 cm^2, Corning). The BG-11 medium was modified as previously reported.[40] Briefly, the HEPES content remained unchanged, while the concentrations of A5 trace metals and other components increased 5- and 2-fold, respectively. $NaHCO_3$ (100 mM) and IPTG (1 mM) were added to the medium. The flasks were shaken horizontally (150 rpm) under continuous light (55 μmol of photons m^{-2} s^{-1}) at 30 °C. On days 1, 2, and 3, cells were collected by centrifugation and resuspended in fresh modified BG-11 medium to an OD_{730} of 3.0. Samples of the cultures were taken every day for measurements.

Quantification of Metabolites. For isopentenol quantification, cell culture was centrifuged for 10 min at 4 °C and 14,000*g*, and isopentenol content in the supernatant was determined by a gas chromatograph (GC) (Agilent model 7890A) equipped with a flame ionization detector. The injection volume is 1 μL. Isopentenol was separated with a HP-5 capillary column (30 m × 0.32 mm internal diameter, 0.25 μm film thickness, Agilent). The GC oven temperature was increased with a gradient of 50 °C min^{-1} from 85 to 150 °C and then 100 °C min^{-1} from 150 to 200 °C.

For pinene quantification, the tetradecane samples were analyzed by a gas chromatograph (GC7890, Agilent) coupled to a mass spectrometer (MS7200QTOF, Agilent). The injection volume is 5 μL. Pinene was separated with a HP-5MS column (30 m × 0.25 mm, 0.25 μm, Agilent). The GC oven temperature started at 50 °C and was increased with a gradient of 3 °C min^{-1} until 70 °C. The temperature of the injector and the ion source of MS was 210 and 230 °C, respectively.

For quantification of intracellular metabolites, cells were harvested at an OD_{730} of ∼1.0. Quenching of metabolism and metabolite extraction were performed as described previously.[56] Briefly, approximately 3 × 10^8 cyanobacterial cells were collected by fast filtration, and metabolites were extracted by rapid transfer of the filter into −20 °C of 80:20 (v/v) methanol/water. After incubation at −20 °C for 20 min, the samples were centrifuged, and the supernatant was collected.

Cell extracts were analyzed by ultrahigh-performance liquid chromatography (UHPLC) (Acquity, Waters) coupled to a quadrupole-orbitrap mass spectrometer (Q-Exactive, Thermo Fisher). Metabolites were separated with a Luna NH2 column (100 × 2 mm^2, 3 μm particle size, Phenomenex). The injection volume was 10 μL. The mobile phase A was 20 mM ammonium acetate in 5% acetonitrile, pH 9.5, and the mobile phase B was acetonitrile. The column was maintained at 15 °C with a solvent flow rate of 0.3 mL min^{-1}, and the gradient of B was as follows: 0 min, 85%; 10 min, 45%; 15 min, 2%; 18 min, 2%; 18.1 min, 85%; 24 min 85% B. The mass spectrometer was run in electrospray ionization negative (ESI^-) mode. The parameters of the mass spectrometer were set as follows: ion spray voltage, +3.8/−3.0 kV; capillary temperature, 320 °C; probe heater temperature, 350 °C; sheath and auxiliary gas, 35 and 10 arbitrary units, respectively. Mass spectra were acquired using a full scan over 70−1000 m/z at 70,000 resolution. This method was used to generate data on the central carbon metabolites. Metabolite identification was performed by matching the retention time, accurate mass, and MS/MS spectra with commercially available standards (Sigma-Aldrich).

MEP pathway intermediates were analyzed by a Q-TRAP mass spectrometer (5500, AB Sciex) equipped with UHPLC (ExionLC AD, AB Sciex) and an XSelect HSS T3 column (100 mm × 3.0 mm, 2.5 μm, Waters). The injection volume was 1 μL. The mobile phase A was 2 mM ammonium bicarbonate and B was methanol. The column was maintained at 40 °C with a flow rate of 0.4 mL min^{-1}, and the gradient of B was as follows: 0 min, 1%; 2 min, 1%; 4 min, 20%; 6 min, 80%; 8 min, 99%; 8.1 min, 1%; 10 min, 1% B. The mass spectrometer was run in ESI^- mode. Data were acquired using the multiple-reaction monitoring mode for the precursor−product ion pairs. The parameters of the mass spectrometer were set as follows: ion spray voltage, −4.5 kV; ion spray temperature, 500 °C; curtain gas, 35 psi; nebulizer gas, 55 psi; heater gas, 55 psi. The compound identities were verified by mass and retention time matches to authenticated standards (Sigma-Aldrich). Metabolite concentrations were determined using a calibration curve generated with varying concentrations of the chemical standard.

^{13}C-Labeling Experiments. The labeling compounds including ^{13}C-labeled $NaHCO_3$ ([^{13}C]bicarbonate) and uniformly ^{13}C-labeled glucose ([*U*-^{13}C]glucose) were ≥99% pure and purchased from Sigma-Aldrich. Cyanobacterial cells were grown in shake flasks with 100 mL of BG-11 medium under continuous light (55 μmol of photons m^{-2} s^{-1}) to an OD_{730} of ∼0.5. After the addition of 1 mM IPTG, the cultures were grown to an OD_{730} of ∼0.8. For [^{13}C]bicarbonate experiments, the culture with constant illumination was supplemented with 1 g L^{-1} of [^{13}C]bicarbonate. For [*U*-^{13}C]glucose experiments, the culture was supplemented with 5 g L^{-1} of [*U*-^{13}C]glucose in the dark. The dark condition was used to reduce the dilution of ^{13}C label in central metabolites from CO_2. At various time points after the isotope addition, cells were collected by fast filtration for LC-MS

https://doi.org/10.1021/acssynbio.3c00675
ACS Synth. Biol. 2024, 13, 876−887

analysis of the labeling of metabolites. Central carbon metabolites and DXP reached an isotopic steady state within 4 min in the [^{13}C]bicarbonate experiment and within 4 h in the [*U*-^{13}C]glucose experiment. The LC-MS data were analyzed as described previously.[56] Briefly, mass isotopomer distributions (MIDs) of metabolites were calculated from measured peak areas of the mass spectra and corrected for naturally occurring ^{13}C. The steady-state ^{13}C enrichment of a metabolite was calculated from the MID according to $\sum_{i=0}^{n} i \cdot m_i/n$,[57] where n is the number of carbon atoms in the metabolite and m_i is the fractional abundance of the ith mass isotopomer.

■ ASSOCIATED CONTENT

Supporting Information

The Supporting Information is available free of charge at https://pubs.acs.org/doi/10.1021/acssynbio.3c00675.

Table of plasmids used in this study; the overall equations of conversion of CO_2 to DXP through the CB cycle and the conventional MEP pathway or the Ru5P shunt; SDS-PAGE of purified recombinant RibB proteins; validation of recombinant *S. elongatus* strains by PCR; and effect of DXS overexpression on intracellular metabolite concentrations (PDF)

■ AUTHOR INFORMATION

Corresponding Author

Chen Yang − *CAS-Key Laboratory of Synthetic Biology, Key Laboratory of Plant Carbon Capture, CAS Center for Excellence in Molecular Plant Sciences, Shanghai Institute of Plant Physiology and Ecology, Chinese Academy of Sciences, Shanghai 200032, China;* orcid.org/0009-0002-1447-9617; Phone: +86-21-54924152; Email: cyang@cemps.ac.cn

Authors

Jie Zhou − *CAS-Key Laboratory of Synthetic Biology, Key Laboratory of Plant Carbon Capture, CAS Center for Excellence in Molecular Plant Sciences, Shanghai Institute of Plant Physiology and Ecology, Chinese Academy of Sciences, Shanghai 200032, China; University of Chinese Academy of Sciences, Beijing 100049, China*

Suxian Xu − *CAS-Key Laboratory of Synthetic Biology, Key Laboratory of Plant Carbon Capture, CAS Center for Excellence in Molecular Plant Sciences, Shanghai Institute of Plant Physiology and Ecology, Chinese Academy of Sciences, Shanghai 200032, China; University of Chinese Academy of Sciences, Beijing 100049, China;* orcid.org/0009-0003-7383-9747

Hu Li − *CAS-Key Laboratory of Synthetic Biology, Key Laboratory of Plant Carbon Capture, CAS Center for Excellence in Molecular Plant Sciences, Shanghai Institute of Plant Physiology and Ecology, Chinese Academy of Sciences, Shanghai 200032, China; University of Chinese Academy of Sciences, Beijing 100049, China;* orcid.org/0009-0000-9721-3923

Huachao Xi − *CAS-Key Laboratory of Synthetic Biology, Key Laboratory of Plant Carbon Capture, CAS Center for Excellence in Molecular Plant Sciences, Shanghai Institute of Plant Physiology and Ecology, Chinese Academy of Sciences, Shanghai 200032, China; University of Chinese Academy of Sciences, Beijing 100049, China;* orcid.org/0009-0007-2414-7188

Wenbo Cheng − *CAS-Key Laboratory of Synthetic Biology, Key Laboratory of Plant Carbon Capture, CAS Center for Excellence in Molecular Plant Sciences, Shanghai Institute of Plant Physiology and Ecology, Chinese Academy of Sciences, Shanghai 200032, China; University of Chinese Academy of Sciences, Beijing 100049, China;* orcid.org/0009-0006-0766-6763

Complete contact information is available at: https://pubs.acs.org/10.1021/acssynbio.3c00675

Author Contributions

J.Z. and C.Y. designed experiments. J.Z. performed most of the experiments. S.X. and H.L. conducted ^{13}C-labeling experiments. H.X. carried out homology modeling of RibB. W.C. contributed to laboratory evolution experiments. J.Z., S.X., and C.Y. analyzed data and wrote the manuscript.

Notes

The authors declare no competing financial interest.

■ ACKNOWLEDGMENTS

The authors would like to thank S. Yang for providing pTrc99A-spec and pCas plasmids and W. Hu and Y. Gao for technical assistance on GC-MS and hybrid quadrupole-orbitrap MS. This work was supported by the National Key Research and Development Program of China (2021YFA0909700), the National Natural Science Foundation of China (31925001, 31921006, and 32230060), and the Chinese Academy of Sciences (XDB27020000).

■ REFERENCES

(1) Gershenzon, J.; Dudareva, N. The function of terpene natural products in the natural world. *Nat. Chem. Biol.* **2007**, *3*, 408−414.

(2) Christianson, D. W. Structural and chemical biology of terpenoid cyclases. *Chem. Rev.* **2017**, *117*, 11570−11648.

(3) Ajikumar, P. K.; Tyo, K.; Carlsen, S.; Mucha, O.; Phon, T. H.; Stephanopoulos, G. Terpenoids: opportunities for biosynthesis of natural product drugs using engineered microorganisms. *Mol. Pharmaceutics* **2008**, *5*, 167−190.

(4) Pahima, E.; Hoz, S.; Ben-Tzion, M.; Major, D. T. Computational design of biofuels from terpenes and terpenoids. *Sustainable Energy Fuels* **2019**, *3*, 457−466.

(5) Chou, H. H.; Keasling, J. D. Synthetic pathway for production of five-carbon alcohols from isopentenyl diphosphate. *Appl. Environ. Microbiol.* **2012**, *78*, 7849−7855.

(6) Yang, Y.; Dec, J. E.; Nicolas, D.; Blake, S. Characteristics of isopentanol as a fuel for HCCI engines. *SAE Int. J. Fuels Lubr.* **2010**, *3*, 725−741.

(7) Harvey, B. G.; Wright, M. E.; Quintana, R. L. High-density renewable fuels based on the selective dimerization of pinenes. *Energy Fuels* **2010**, *24*, 267−273.

(8) Miziorko, H. M. Enzymes of the mevalonate pathway of isoprenoid biosynthesis. *Arch. Biochem. Biophys.* **2011**, *505*, 131−143.

(9) Lange, B. M.; Rujan, T.; Martin, W.; Croteau, R. Isoprenoid biosynthesis: the evolution of two ancient and distinct pathways across genomes. *Proc. Natl. Acad. Sci. U.S.A.* **2000**, *97*, 13172−13177.

(10) Davies, F. K.; Jinkerson, R. E.; Posewitz, M. C. Toward a photosynthetic microbial platform for terpenoid engineering. *Photosynth. Res.* **2015**, *123*, 265−284.

(11) Ni, J.; Tao, F.; Xu, P.; Yang, C.Engineering Cyanobacteria for Photosynthetic Production of C3 Platform Chemicals and Terpenoids from CO_2. In *Synthetic Biology of Cyanobacteria*, Advances in Experimental Medicine and Biology; Springer, 2018; Vol. *1080*, pp 239−259.

(12) Lindberg, P.; Park, S.; Melis, A. Engineering a platform for photosynthetic isoprene production in cyanobacteria, using *Synechocystis* as the model organism. *Metab. Eng.* **2010**, *12*, 70−79.
(13) Gao, X.; Gao, F.; Liu, D.; Zhang, H.; Nie, X.; Yang, C. Engineering the methylerythritol phosphate pathway in cyanobacteria for photosynthetic isoprene production from CO_2. *Energy Environ. Sci.* **2016**, *9*, 1400−1411.
(14) Halfmann, C.; Gu, L.; Zhou, R. Engineering cyanobacteria for the production of a cyclic hydrocarbon fuel from CO_2 and H_2O. *Green Chem.* **2014**, *16*, 3175−3185.
(15) Davies, F. K.; Work, V. H.; Beliaev, A. S.; Posewitz, M. C. Engineering limonene and bisabolene production in wild type and a glycogen-deficient mutant of *Synechococcus* sp. PCC 7002. *Front. Bioeng. Biotechnol.* **2014**, *2*, No. 21.
(16) Halfmann, C.; Gu, L.; Gibbons, W.; Zhou, R. Genetically engineering cyanobacteria to convert CO_2, water, and light into the long-chain hydrocarbon farnesene. *Appl. Microbiol. Biotechnol.* **2014**, *98*, 9869−9877.
(17) Choi, S. Y.; Lee, H. J.; Choi, J.; Kim, J.; Sim, S. J.; Um, Y.; Kim, Y.; Lee, T. S.; Keasling, J. D.; Woo, H. M. Photosynthetic conversion of CO_2 to farnesyl diphosphate-derived phytochemicals (amorpha-4,11-diene and squalene) by engineered cyanobacteria. *Biotechnol. Biofuels* **2016**, *9*, No. 202.
(18) Englund, E.; Pattanaik, B.; Ubhayasekera, S. J. K.; Stensjö, K.; Bergquist, J.; Lindberg, P. Production of squalene in *Synechocystis* sp. PCC 6803. *PloS One* **2014**, *9* (3), No. e90270.
(19) Choi, S. Y.; Wang, J.-Y.; Kwak, H. S.; Lee, S.-M.; Um, Y.; Kim, Y.; Sim, S. J.; Choi, J.-I.; Woo, H. M. Improvement of squalene production from CO_2 in *Synechococcus elongatus* PCC 7942 by metabolic engineering and scalable production in a photobioreactor. *ACS Synth. Biol.* **2017**, *6*, 1289−1295.
(20) Banerjee, A.; Sharkey, T. D. Methylerythritol 4-phosphate (MEP) pathway metabolic regulation. *Nat. Prod. Rep.* **2014**, *31*, 1043−1055.
(21) Farmer, W. R.; Liao, J. C. Precursor balancing for metabolic engineering of lycopene production in *Escherichia coli*. *Biotechnol. Prog.* **2001**, *17*, 57−61.
(22) Jung, J.; Lim, J. H.; Kim, S. Y.; Im, D. K.; Seok, J. Y.; Lee, S. V.; Oh, M. K.; Jung, G. Y. Precise precursor rebalancing for isoprenoids production by fine control of *gapA* expression in *Escherichia coli*. *Metab. Eng.* **2016**, *38*, 401−408.
(23) Sauret-Güeto, S.; Urós, E. M.; Ibáñez, E.; Boronat, A.; Rodríguez-Concepción, M. A mutant pyruvate dehydrogenase E1 subunit allows survival of *Escherichia coli* strains defective in 1-deoxy-D-xylulose 5-phosphate synthase. *FEBS Lett.* **2006**, *580*, 736−740.
(24) Perez-Gil, J.; Uros, E. M.; Sauret-Güeto, S.; Lois, L. M.; Kirby, J.; Nishimoto, M.; Baidoo, E. E.; Keasling, J. D.; Boronat, A.; Rodriguez-Concepcion, M. Mutations in *Escherichia coli* aceE. *PloS One* **2012**, *7*, No. e43775.
(25) Kirby, J.; Nishimoto, M.; Chow, R. W.; Baidoo, E. E.; Wang, G.; Martin, J.; Schackwitz, W.; Chan, R.; Fortman, J. L.; Keasling, J. D. Enhancing terpene yield from sugars via novel routes to 1-deoxy-D-xylulose 5-phosphate. *Appl. Environ. Microbiol.* **2015**, *81*, 130−138.
(26) Hernandez-Arranz, S.; Perez-Gil, J.; Marshall-Sabey, D.; Rodriguez-Concepcion, M. Engineering *Pseudomonas putida* for isoprenoid production by manipulating endogenous and shunt pathways supplying precursors. *Microb. Cell Fact.* **2019**, *18*, No. 152.
(27) Kudoh, K.; Kubota, G.; Fujii, R.; Kawano, Y.; Ihara, M. Exploration of the 1-deoxy-D-xylulose 5-phosphate synthases suitable for the creation of a robust isoprenoid biosynthesis system. *J. Biosci. Bioeng.* **2017**, *123*, 300−307.
(28) Yokota, A.; Sasajima, K.-I. Formation of 1-deoxy-ketoses by pyruvate dehydrogenase and acetoin dehydrogenase. *Agric. Biol. Chem.* **1986**, *50*, 2517−2524.
(29) Antonovsky, N.; Gleizer, S.; Noor, E.; Zohar, Y.; Herz, E.; Barenholz, U.; Zelcbuch, L.; Amram, S.; Wides, A.; Tepper, N.; Davidi, D.; Bar-On, Y.; Bareia, T.; Wernick, D. G.; Shani, I.; Malitsky, S.; Jona, G.; Bar-Even, A.; Milo, R. Sugar synthesis from CO_2 in *Escherichia coli*. *Cell.* **2016**, *166*, 115−125.
(30) Gleizer, S.; Ben-Nissan, R.; Bar-On, Y. M.; Antonovsky, N.; Noor, E.; Zohar, Y.; Jona, G.; Krieger, E.; Shamshoum, M.; Bar-Even, A.; Milo, R. Conversion of *Escherichia coli* to generate all biomass carbon from CO_2. *Cell* **2019**, *179*, 1255−1263.
(31) Richter, G.; Volk, R.; Krieger, C.; Lahm, H. W.; Rothlisberger, U.; Bacher, A. Biosynthesis of riboflavin: cloning, sequencing, and expression of the gene coding for 3,4-dihydroxy-2-butanone 4-phosphate synthase of *Escherichia coli*. *J. Bacteriol.* **1992**, *174*, 4050−4056.
(32) Islam, Z.; Kumar, A.; Singh, S.; Salmon, L.; Karthikeyan, S. Structural basis for competitive inhibition of 3,4-dihydroxy-2-butanone-4-phosphate synthase from *Vibrio cholerae*. *J. Biol. Chem.* **2015**, *290*, 11293−11308.
(33) Shinde, R. N.; Karthikeyan, S.; Singh, B. Molecular dynamics studies unravel role of conserved residues responsible for movement of ions into active site of DHBPS. *Sci. Rep.* **2017**, *7*, No. 40452.
(34) Steinbacher, S.; Schiffmann, S.; Richter, G.; Huber, R.; Bacher, A.; Fischer, M. Structure of 3,4-dihydroxy-2-butanone 4-phosphate synthase from *Methanococcus jannaschii* in complex with divalent metal ions and the substrate ribulose 5-phosphate: implications for the catalytic mechanism. *J. Biol. Chem.* **2003**, *278*, 42256−42265.
(35) Young, J. D.; Shastri, A. A.; Stephanopoulos, G.; Morgan, J. A. Mapping photoautotrophic metabolism with isotopically nonstationary ^{13}C flux analysis. *Metab. Eng.* **2011**, *13*, 656−665.
(36) Hendry, J. I.; Prasannan, C.; Ma, F.; Möllers, K. B.; Jaiswal, D.; Digmurti, M.; Allen, D. K.; Frigaard, N. U.; Dasgupta, S.; Wangikar, P. P. Rerouting of carbon flux in a glycogen mutant of cyanobacteria assessed via isotopically non-stationary ^{13}C metabolic flux analysis. *Biotechnol. Bioeng.* **2017**, *114*, 2298−2308.
(37) McEwen, J. T.; Machado, I. M.; Connor, M. R.; Atsumi, S. Engineering *Synechococcus elongatus* PCC 7942 for continuous growth under diurnal conditions. *Appl. Environ. Microbiol.* **2013**, *79*, 1668−1675.
(38) You, L.; He, L.; Tang, Y. J. Photoheterotrophic fluxome in *Synechocystis* sp. strain PCC 6803 and its implications for cyanobacterial bioenergetics. *J. Bacteriol.* **2015**, *197*, 943−950.
(39) You, L.; Berla, B.; He, L.; Pakrasi, H. B.; Tang, Y. J. ^{13}C-MFA delineates the photomixotrophic metabolism of *Synechocystis* sp. PCC 6803 under light- and carbon-sufficient conditions. *Biotechnol. J.* **2014**, *9*, 684−692.
(40) Kanno, M.; Carroll, A. L.; Atsumi, S. Global metabolic rewiring for improved CO_2 fixation and chemical production in cyanobacteria. *Nat. Commun.* **2017**, *8*, No. 14724.
(41) Wang, T.; Zhu, H.; Yang, C. Development of CRISPRa for metabolic engineering applications in cyanobacteria. *Synth. Biol. J.* **2023**, *4*, 824−839.
(42) Sarria, S.; Wong, B.; Martín, H. G.; Keasling, J. D.; Peralta-Yahya, P. Microbial synthesis of pinene. *ACS Synth. Biol.* **2014**, *3*, 466−475.
(43) Tashiro, M.; Kiyota, H.; Kawai-Noma, S.; Saito, K.; Ikeuchi, M.; Iijima, Y.; Umeno, D. Bacterial production of pinene by a laboratory-evolved pinene-synthase. *ACS Synth. Biol.* **2016**, *5*, 1011−1020.
(44) Harpel, M. R.; Larimer, F. W.; Hartman, F. C. Multifaceted roles of Lys166 of ribulose-bisphosphate carboxylase/oxygenase as discerned by product analysis and chemical rescue of site-directed mutants. *Biochemistry* **2002**, *41*, 1390−1397.
(45) Li, Q.; Fan, F.; Gao, X.; Yang, C.; Bi, C.; Tang, J.; Liu, T.; Zhang, X. Balanced activation of IspG and IspH to eliminate MEP intermediate accumulation and improve isoprenoids production in *Escherichia coli*. *Metab. Eng.* **2017**, *44*, 13−21.
(46) Nguyen, A. D.; Pham, D. N.; Chau, T. H. T.; Lee, E. Y. Enhancing sesquiterpenoid production from methane via synergy of the methylerythritol phosphate pathway and a short-cut route to 1-deoxy-D-xylulose 5-phosphate in methanotrophic bacteria. *Microorganisms* **2021**, *9*, No. 1236.
(47) Lv, Y.; Qian, S.; Du, G.; Chen, J.; Zhou, J.; Xu, P. Coupling feedback genetic circuits with growth phenotype for dynamic

population control and intelligent bioproduction. *Metab. Eng.* **2019**, *54*, 109−116.
(48) Jiang, Y.; Chen, B.; Duan, C.; Sun, B.; Yang, J.; Yang, S. Multigene editing in the *Escherichia coli* genome via the CRISPR-Cas9 system. *Appl. Environ. Microbiol.* **2015**, *81*, 2506−2514.
(49) Mackey, S. R.; Ditty, J. L.; Clerico, E. M.; Golden, S. S.Detection of Rhythmic Bioluminescence from Luciferase Reporters in Cyanobacteria. In *Circadian Rhythms*, Methods in Molecular Biology; Springer, 2007; Vol. *362*, pp 115−129.
(50) Andersson, C. R.; Tsinoremas, N. F.; Shelton, J.; Lebedeva, N. V.; Yarrow, J.; Min, H.; Golden, S. S.Application of Bioluminescence to the Study of Circadian Rhythms in Cyanobacteria. In *Methods in Enzymology*; Elsevier, 2000; Vol. *305*, pp 527−542.
(51) Oliver, J. W. K.; Machado, I. M.; Yoneda, H.; Atsumi, S. Cyanobacterial conversion of carbon dioxide to 2,3-butanediol. *Proc. Natl. Acad. Sci. U.S.A.* **2013**, *110*, 1249−1254.
(52) Rippka, R.; Deruelles, J.; Waterbury, J. B.; Herdman, M.; Stanier, R. Y. Generic assignments, strain histories and properties of pure cultures of cyanobacteria. *Microbiology* **1979**, *111*, 1−61.
(53) Yang, C.; Gao, X.; Jiang, Y.; Sun, B.; Gao, F.; Yang, S. Synergy between methylerythritol phosphate pathway and mevalonate pathway for isoprene production in *Escherichia coli*. *Metab. Eng.* **2016**, *37*, 79−91.
(54) Yang, C.; Rodionov, D. A.; Rodionova, I. A.; Li, X.; Osterman, A. L. Glycerate 2-kinase of *Thermotoga maritima* and genomic reconstruction of related metabolic pathways. *J. Bacteriol.* **2008**, *190*, 1773−1782.
(55) George, K. W.; Thompson, M. G.; Kang, A.; Baidoo, E.; Wang, G.; Chan, L. J.; Adams, P. D.; Petzold, C. J.; Keasling, J. D.; Lee, T. S. Metabolic engineering for the high-yield production of isoprenoid-based C_5 alcohols in *E. coli*. *Sci. Rep.* **2015**, *5*, No. 11128.
(56) Zhang, H.; Liu, Y.; Nie, X.; Liu, L.; Hua, Q.; Zhao, G. P.; Yang, C. The cyanobacterial ornithine-ammonia cycle involves an arginine dihydrolase. *Nat. Chem. Biol.* **2018**, *14*, 575−581.
(57) Yuan, J.; Bennett, B. D.; Rabinowitz, J. D. Kinetic flux profiling for quantitation of cellular metabolic fluxes. *Nat. Protoc.* **2008**, *3*, 1328−1340.

https://doi.org/10.1021/acssynbio.3c00675
ACS Synth. Biol. 2024, 13, 876−887